

## ANALYSIS OF FRICTION EFFECTS IN THE STRUCTURAL BEHAVIOR OF SANDWICH PIPES UNDER AXISYMMETRIC LOADS

Flamínio Alves Fávero Maranhão, [flaminio@usp.br](mailto:flaminio@usp.br)

Roberto Ramos Jr., [rrososjr@usp.br](mailto:rrososjr@usp.br)

Escola Politécnica of the University of São Paulo, Mechanical Engineering Department  
Av. Prof. Mello Moraes, 2231, São Paulo, SP, Brazil, 05508-970

**Abstract.** *This paper presents a study to identify, in a qualitative manner, how friction effects between adjacent layers of concentric pipes affects their global structural behavior when such structures are subjected to axisymmetric loads (traction and uniform pressures), in order to detect some non-linear effects. Pipe-in-pipe models are analyzed, through simplified analytical formulations and then through finite element simulations, considering no initial gaps between adjacent layers and using a simple Coulomb dry friction model. Through the simulations, the values for the equivalent axial stiffness are obtained and compared to that predicted by the analytical model and the results are discussed.*

**Keywords:** *pipe-in-pipe, sandwich pipes, finite element analysis, contact, friction*

### 1. INTRODUCTION

Pipe-in-Pipe systems, also known as sandwich pipes, are structures that consist basically of two concentric metal tubes, fulfilled with a non-structural thermal-resistant material. They can be used for deepwater oil and gas transportation, combining structural resistance with thermal insulation characteristics. Figure 1 presents a typical sandwich pipe construction. Several researches have been recently carried out in order to investigate the behavior of these elements, mainly regarding their structural instability (see, e.g., Castello and Estefen (2007) and Estefen et al.(2005)).



Figure 1. A sandwich pipe construction (Estefen et al (2005)).

One important step for a pipe design is to predict the global behavior of the sandwich pipe under certain loads. Simplified analytical models may be used to make such a prediction, based on some hypotheses which may (or may not) be restrictive. One of the most usual hypotheses is the one that considers that all the adjacent tubes are perfectly bonded and that there is no friction between the internal layers. However, it is interesting to verify how those effects might affect the global behavior of the sandwich pipe. In this paper, a simplified analytical model will be first proposed to predict the behavior of the whole pipe under internal and external pressures and traction loads, as well as the value of the equivalent axial stiffness of the pipe. Then some finite element analyses are performed, disregarding some of the hypotheses used in the analytical model, in order to compare the results obtained.

### 2. SIMPLIFIED ANALYTICAL MODELS

In this section some simplified analytical models derived from the classical theory of elasticity (see, e.g., Timoshenko and Goodier (1980), Sokolnikoff (1956) or Love (1944)) will be presented. The results obtained through these simplified models, such as the equivalent axial stiffness values, will be used as a comparative basis for the numerical simulation results obtained through finite element models. The following hypotheses will be assumed in the derivation of the analytical models:

- i) all materials are homogeneous;
- ii) all materials have a linear-elastic behavior;
- iii) all materials are isotropic;
- iv) the sections which were plane before deformation remain plane after deformation;
- v) all layers are considered as having perfectly concentric cylindrical surfaces;
- vi) all the adjacent layers are perfectly bonded together;
- vii) geometric linearity applies;
- viii) friction forces between adjacent layers can be neglected;
- ix) in the extreme cross-sections all the layers are subjected to the same axial displacement

**2.1. Analytical model for traction and internal/external pressures loads**

Let us consider a sandwich pipe construction formed by the superposition on  $n$  concentric pipes numbered from  $j=1$  (most internal pipe) to  $j=n$  (most external pipe) as depicted in Fig. 2 for the case of a sandwich pipe with three layers. Let  $L_o$  be the total initial (non-deformed) length of this structure,  $R_{i,j}$  and  $R_{o,j}$  the initial (non-deformed) values for the internal and external radius for the  $j$ -th layer, respectively, and  $E_j, G_j, \lambda_j$  and  $\nu_j$  the elastic constants for the  $j$ -th layer.

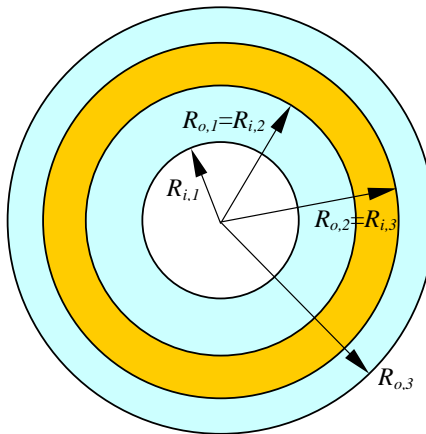


Figure 2. A schematic sandwich pipe cross-section with three layers.

Considering the aforementioned set of hypotheses it is possible to show that the solution for the radial displacement functions for each layer is given by:

$$u_{r,j} = C_{1,j} \cdot r + \frac{C_{2,j}}{r}, \quad 1 \leq j \leq n \tag{1}$$

where the constants  $C_{1,j}$  and  $C_{2,j}$  for the  $j$ -th layer are functions of: layer geometry ( $R_{i,j}$  and  $R_{o,j}$ ); elastic constants (e.g.,  $E_j, G_j, \lambda_j$  and  $\nu_j$ ); internal and external pressures acting in the layer ( $p_{i,j}$  and  $p_{o,j}$ ) and longitudinal strain  $\varepsilon_z$ , which is the same for all layers. Figure 3 shows the loading considered for each layer.

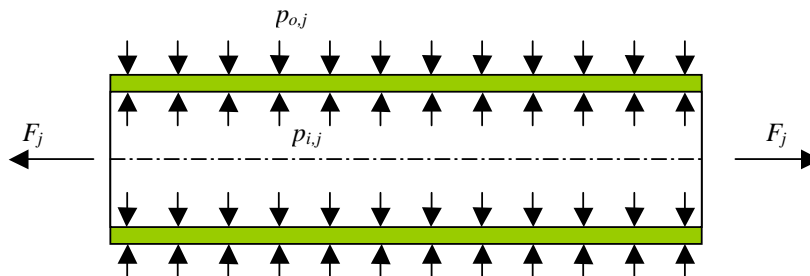


Figure 3. Loading supported for the  $j$ -th layer.

The total number of unknowns for this problem is then  $5n + 1$ , which are defined according to Table 1.

Table 1. Unknowns of the problem.

Unknown	Description	Number of unknowns
$C_{1,j}, C_{2,j}$	integration constants for the $j$ -th layer	$2n$
$p_{i,j}, p_{o,j}$	internal and external pressures in the $j$ -th layer	$2n$
$F_j$	axial force in the $j$ -th layer	$n$
$\varepsilon_z$	axial strain in the pipe	1
<b>Total of unknowns</b>		<b><math>5n + 1</math></b>

All these  $5n + 1$  unknowns can be obtained through the solution of a linear system given by  $5n + 1$  independent equations which comprises:

- a)  $(2n)$  boundary conditions related to the internal and external pressures in each layer given by:

$$\lambda_j \cdot (2C_{1,j} + \varepsilon_z) + 2G_j \cdot \left( C_{1,j} - \frac{C_{2,j}}{R_{i,j}^2} \right) = -p_{ij} \quad (1 \leq j \leq n) \quad (2)$$

$$\lambda_j \cdot (2C_{1,j} + \varepsilon_z) + 2G_j \cdot \left( C_{1,j} - \frac{C_{2,j}}{R_{o,j}^2} \right) = -p_{oj}$$

- b)  $(n - 1)$  compatibility equations applied to each of the  $(n - 1)$  interfaces between adjacent layers given by:

$$C_{1,j} \cdot R_{o,j} + \frac{C_{2,j}}{R_{o,j}} = C_{1,j+1} \cdot R_{o,j+1} + \frac{C_{2,j+1}}{R_{o,j+1}} \quad (1 \leq j \leq n-1) \quad (3)$$

- c)  $(n)$  equilibrium equations for the axial forces in each layer given by:

$$F_j = \pi(R_{o,j}^2 - R_{i,j}^2) \cdot \left[ \lambda_j \cdot (2C_{1,j} + \varepsilon_z) + 2G_j \cdot \varepsilon_z \right] \quad (4)$$

- d)  $(n + 1)$  compatibility equations for the pressures at the interfaces between adjacent layers given by:

$$\begin{cases} p_{o,j} = p_{i,j+1} & (1 \leq j \leq n-1) \\ p_{i,1} = p_i = \text{internal pressure in the pipe} \\ p_{o,n} = p_o = \text{external pressure in the pipe} \end{cases} \quad (5)$$

- e) (1) axial force equilibrium equation for the set of layers which is given by:

$$\sum_{j=1}^n F_j = F = \text{total force applied to the pipe} \quad (6)$$

Considering that the pipe has an initial length  $L_o$ , the internal and external pressures applied to its internal and external lateral surfaces can be related to forces  $F_{pi}$  and  $F_{po}$  defined respectively by:

$$F_{pi} = \iint_{A_i} p_i \cdot dA = p_i 2\pi R_{i,1} L_o$$

$$F_{po} = -\iint_{A_o} p_o \cdot dA = -p_o 2\pi R_{o,n} L_o \quad (7)$$

## 2.1. Global Stiffness Matrix and Coupling Effects

If we consider as global input parameters for the loads applied to the pipe: the total axial force  $F$  applied to its cross-section and the two forces  $F_{pi}$  and  $F_{po}$  applied to its lateral surfaces, the following relationship between forces and displacements can be derived, after one obtains the complete solution for the  $5n + 1$  unknowns given in Tab.1 (see also Ramos et al. (2008)):

$$\begin{bmatrix} k_{11} & k_{12} & k_{13} \\ k_{21} & k_{22} & k_{23} \\ k_{31} & k_{32} & k_{33} \end{bmatrix} \cdot \begin{bmatrix} \Delta L \\ \Delta R_i \\ \Delta R_o \end{bmatrix} = \begin{bmatrix} F \\ F_{pi} \\ F_{po} \end{bmatrix} \quad (8)$$

where  $k_{ij}$  is the corresponding component for the stiffness matrix  $[K]$ ,  $\Delta L$  is the change in length of the pipe, and  $\Delta R_i = u_{r,1}(R_{i,1})$  and  $\Delta R_o = u_{r,n}(R_{o,n})$  are the displacements for the internal and external surfaces of the pipe, respectively. If we solve the system of equations given by Eq.(8) for the unknowns  $\Delta L$ ,  $\Delta R_i$  and  $\Delta R_o$ , it is straightforward to show that:

$$\Delta L = \frac{1}{\det(K)} \det \begin{bmatrix} F & k_{12} & k_{13} \\ F_{pi} & k_{22} & k_{23} \\ F_{po} & k_{32} & k_{33} \end{bmatrix}, \quad \Delta R_i = \frac{1}{\det(K)} \det \begin{bmatrix} k_{11} & F & k_{13} \\ k_{21} & F_{pi} & k_{23} \\ k_{31} & F_{po} & k_{33} \end{bmatrix}, \quad \Delta R_o = \frac{1}{\det(K)} \det \begin{bmatrix} k_{11} & k_{12} & F \\ k_{21} & k_{22} & F_{pi} \\ k_{31} & k_{32} & F_{po} \end{bmatrix} \quad (9)$$

which is equivalent to:

$$\begin{aligned} \Delta L &= \left( \frac{k_{22} \cdot k_{33} - k_{23} \cdot k_{32}}{\det(K)} \right) \cdot F + \left( \frac{k_{13} \cdot k_{32} - k_{12} \cdot k_{33}}{\det(K)} \right) \cdot F_{pi} + \left( \frac{k_{12} \cdot k_{23} - k_{13} \cdot k_{22}}{\det(K)} \right) \cdot F_{po} \\ \Delta R_i &= \left( \frac{k_{23} \cdot k_{31} - k_{21} \cdot k_{33}}{\det(K)} \right) \cdot F + \left( \frac{k_{11} \cdot k_{33} - k_{13} \cdot k_{31}}{\det(K)} \right) \cdot F_{pi} + \left( \frac{k_{13} \cdot k_{21} - k_{11} \cdot k_{23}}{\det(K)} \right) \cdot F_{po} \\ \Delta R_o &= \left( \frac{k_{21} \cdot k_{32} - k_{22} \cdot k_{31}}{\det(K)} \right) \cdot F + \left( \frac{k_{12} \cdot k_{31} - k_{11} \cdot k_{32}}{\det(K)} \right) \cdot F_{pi} + \left( \frac{k_{11} \cdot k_{22} - k_{12} \cdot k_{21}}{\det(K)} \right) \cdot F_{po} \end{aligned} \quad (10)$$

## 2.2. Equivalent Axial Stiffness

A usual and very simple way to define the equivalent axial stiffness for a set of pipes comes from the equation:

$$F = \sum_{i=1}^N (E_i A_i) \cdot \varepsilon_z = (EA)_{eq} \cdot \varepsilon_z \quad (11)$$

where  $E_i$  is the modulus of elasticity of the  $i$ -th layer,  $A_i$  is the cross-section area of the  $i$ -th layer and  $\varepsilon_z$  is the axial deformation. It is important to emphasize, however, that Eq. (11) does not consider any kind of interaction between the adjacent layers, but Eqs. (10) do consider. So, from Eq.(10-a), it follows that:

$$F = \left( \frac{\det(K)}{k_{22} \cdot k_{33} - k_{23} \cdot k_{32}} \right) \Delta L + \left( \frac{k_{12} \cdot k_{33} - k_{13} \cdot k_{32}}{k_{22} \cdot k_{33} - k_{23} \cdot k_{32}} \right) \cdot F_{pi} + \left( \frac{k_{13} \cdot k_{22} - k_{12} \cdot k_{23}}{k_{22} \cdot k_{33} - k_{23} \cdot k_{32}} \right) \cdot F_{po} \quad (12)$$

This is similar to Eq. (11) except by the terms that depend on  $F_{pi}$  and  $F_{po}$ . Now, if we remember that  $\Delta L = L_o \cdot \varepsilon_z$ , we can define the true equivalent axial stiffness of the pipe-in-pipe system as the one given by:

$$(EA)_{eq} = \left( \frac{\det(K) \cdot L_o}{k_{22} \cdot k_{33} - k_{23} \cdot k_{32}} \right) \quad (13)$$

### 3. FINITE ELEMENT MODEL

The terms  $k_{ij}$  given in Eq. (8) can be obtained analytically as shown in the previous section, considering the hypotheses used in the derivation. However, it is interesting to obtain numerically the values  $k_{ij}$ , disregarding some of the hypotheses used, and compare the obtained values.

In order to obtain those values for matrix  $K$ , some finite element analyses have been performed. The finite element models were built in MSC.Patran® and simulated in MSC.Marc®. A three-layer sandwich pipe, as described in Table 2, with size  $L_0 = 1000$  mm, was modeled, following the geometry of the sandwich pipe studied by Estefen et al (2005). Since both geometry and loadings are axisymmetric, so are the results, leading to the choice of planar axisymmetric linear elements to perform the analyses. This approach greatly reduced the computation time if compared to that of a full 3D-modeling.

Table 2. Description of the model layers.

Layer	Internal radius	External Radius	Material	Modulus of Elasticity	Poisson Coefficient
1	25 mm	27 mm	Aluminum	70 GPa	0.29
2	27 mm	38 mm	Polypropylene	10 GPa	0.34
3	38 mm	40 mm	Aluminum	70 GPa	0.29

In order to check for the relative importance of non-linear effects in the global structural behavior, three different cases were studied in the FE analyses:

- Case 1 – the tubes are perfectly bonded;
- Case 2 – the tubes are unbounded with no friction between the layers;
- Case 3 – the tubes are unbounded with friction between layers.

All three cases were modeled equally, only changing the type of contact between each layer defined in the FE application: Case 1 was modeled as “Glued” contact; Cases 2 and 3 were modeled as “Touch” contact. The friction model used in Case 3 was a simple Coulomb “dry-friction” model. The friction coefficients between all layers were considered to be equal to 0.5.

#### 3.1 Boundary Conditions

All three cases were modeled with two possible end conditions:

- A - The extreme sections are rigid, i.e., the radius can not vary at any point of the pipe ends, and
- B - The extreme sections are free to expand/contract radially, so radial displacements are possible in all sections.

The end condition “A” generates variations in the internal and external radius through the axial coordinate, so in this case the external and internal radius variations were measured in terms of an average value given by:

$$\Delta R_i = \frac{1}{L_0} \int_0^{L_0} \Delta R_i(z) dz \quad , \quad \Delta R_o = \frac{1}{L_0} \int_0^{L_0} \Delta R_o(z) dz \quad (14)$$

The end condition “B”, in conjunction with the boundary condition related to hypothesis (ix), leads to a state in which almost no slip between adjacent layers is possible, that is, to a state which is quite similar to the “plane sections remain plane” hypothesis. So, all three cases with boundary condition “B” yield to almost identical results (irrespective of how the contact and friction between adjacent layers were modeled), since there is practically no slip between layers. As a result of that, the end condition “B”, and all results related to this condition, will be treated as Case 4.

#### 3.2 Finite Element Simulations

The linear system given by Eq. (8) can be expanded to solve three different cases at a time:

$$\begin{bmatrix} k_{11} & k_{12} & k_{13} \\ k_{21} & k_{22} & k_{23} \\ k_{31} & k_{32} & k_{33} \end{bmatrix} \cdot \begin{bmatrix} \Delta L_1 & \Delta L_2 & \Delta L_3 \\ \Delta R_{i,1} & \Delta R_{i,2} & \Delta R_{i,3} \\ \Delta R_{o,1} & \Delta R_{o,2} & \Delta R_{o,3} \end{bmatrix} = \begin{bmatrix} F_1 & F_2 & F_3 \\ F_{pi,1} & F_{pi,2} & F_{pi,3} \\ F_{po,1} & F_{po,2} & F_{po,3} \end{bmatrix} \quad (15)$$

It is possible to solve for the all the nine stiffness coefficients of the matrix  $K$  by running three independent simulations. The FE inputs and its respective results, for each simulation, are used to fill each column of the displacement and force matrices in Eq. (15), and then the matrix  $K$  is determined. The independent variables used in each simulation were:  $\Delta L$ , the total displacement in top section,  $p_i$ , the internal pressure, and  $p_o$ , the external pressure. The results observed through the simulations were:  $F$ , which is the total sum of each layer reaction force,  $R_i$ , the average variation of the internal radius, and  $R_o$ , the average variation of the external radius.

The four cases proposed were simulated that way and the results for each matrix  $K$  are shown in the next section. The hypotheses considered for each case are summarized in Table 3.

Table 3. Hypotheses used in the FE models.

Hypothesis	Analytical	FE Case 1	FE Case 2	FE Case 3	FE Case 4
Homogeneous materials	X	X	X	X	X
Linear-elastic behavior	X	X	X	X	X
Isotropic material	X	X	X	X	X
Plane sections remain plane	X				
Tubes are perfectly bonded	X	X			X
No initial gaps between layers	X	X	X	X	X
Geometric Linearity Applies	X				X
Friction forces can be neglected	X	X	X		X
Same axial displacement on top sections	X	X	X	X	X

#### 4. RESULTS FROM FEA

The analytical solution for  $K$  was obtained in a Maple® routine to solve Eqs. (1-8), whereas the FE simulations provided the values needed to obtain the numerical values of  $k_{ij}$ , for each case considered, as described in Eq. (15). All results are shown in the following sections:

##### 4.1 Values for $k_{ij}$

Tables 4 and 5 present the numerical values for  $k_{ij}$  and relative errors between the FE simulations and the analytical prediction for each case, respectively. The matrix  $K$  obtained analytically is symmetric, and the ones obtained numerically for Cases 1 and 4 are “almost” symmetric, i.e, the terms  $k_{ij}$  and  $k_{ji}$  are nearly close, but not exactly equal. It was not possible to conclude if such lack of symmetry was caused only by numerical effects. Case 4 results are much closer to the analytical ones, when compared to the results of other cases, but that should be expected since Case 4 conditions almost reproduce the set of hypotheses considered in the analytical model. It is interesting to note that the unbounded hypothesis, considered in Cases 2 and 3, introduces a remarkable asymmetry in matrix  $K$ , especially in the terms  $k_{21}$  (error of -24%) and  $k_{31}$  (error of -16%). Moreover, the presence of friction forces introduces a very small difference in those terms, showing that the gap formation effects caused by the unbounding of layers are more relevant than the friction forces in this case.

Table 4. Results for  $k_{ij}$  terms (kN/mm).

	Analytical	Case 1 (Perfectly Bonded)	Case 2 (Unbonded with no friction)	Case 3 (Unbonded with friction, $\mu = 0.5$ )	Case 4 (Plane sections remain plane)
$k_{11}$	0.102	0.102	0.099	0.099	0.102
$k_{12}$	-1.347	-1.355	-1.357	-1.356	-1.347
$k_{13}$	2.607	2.622	2.624	2.622	2.607
$k_{21}$	-1.347	-1.347	-1.029	-1.027	-1.346
$k_{22}$	250.942	254.212	254.343	254.080	251.059
$k_{23}$	-257.507	-260.124	-260.438	-260.066	-257.539
$k_{31}$	2.607	2.607	2.193	2.191	2.605
$k_{32}$	-257.507	-260.124	-260.519	-260.249	-257.637
$k_{33}$	362.509	366.947	367.132	366.752	362.577

Table 5. Relative errors (%) in  $k_{ij}$  terms when compared to the analytical prediction.

	Case 1 (Perfectly Bonded)	Case 2 (Unbonded with no friction)	Case 3 (Unbonded with friction, $\mu = 0.5$ )	Case 4 (Plane sections remain plane)
$k_{11}$	0	-2.94	-2.94	0
$k_{12}$	0.59	0.74	0.67	0
$k_{13}$	0.58	0.65	0.58	0
$k_{21}$	0	-23.61	-23.76	-0.07
$k_{22}$	1.3	1.36	1.25	0.05
$k_{23}$	1.02	1.14	0.99	0.01
$k_{31}$	0	-15.88	-15.96	-0.08
$k_{32}$	1.02	1.17	1.06	0.05
$k_{33}$	1.22	1.28	1.17	0.02

#### 4.2 Comparison of $(EA)_{eq}$

In order to compare the cases, values for the equivalent axial stiffness were calculated, as given in Eq (13). Despite the variations of the  $k_{ij}$  terms between the cases, those values are nearly the same for all of them. The equivalent axial stiffness was also evaluated from Eq. (11), which does not consider any interaction between the layers. Table 6 presents the results and the relative errors using the analytical model (Eq.(13)) as basis.

Table 6. Comparison between  $(EA)_{eq}$  for each case.

	Eq.(11)	Eq.(13)	FE Case 1	FE Case 2	FE Case 3	FE Case 4
$(EA)_{eq}$ (kN)	79.639 E3	79.688 E3	79.861 E3	79.757 E3	79.757 E3	79.599 E3
Error (%)	-0.06	0	0.21	0.08	0.08	-0.11

#### 4.3 Contact effects

Cases 2 and 3 present some results that could not be obtained using the analytical model proposed: variations in the internal and external radius, gap formation and friction effects. It is interesting to note that those effects happen only near the top sections. The results for a displacement of 1 mm (related to an average axial strain  $\bar{\epsilon}_z = 0,1\%$ ), with neither internal nor external pressures applied, are shown in Fig. 4, 5 and 6.

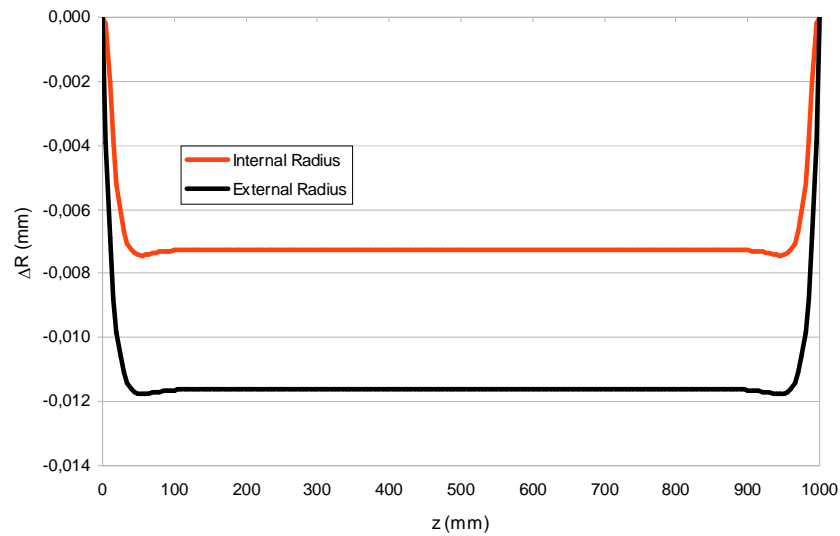


Figure 4. Radius variation along the length in a sandwich pipe submitted to traction load (Case 3).

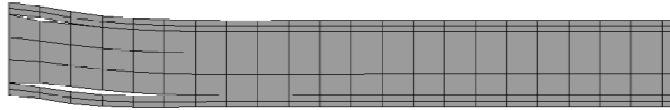


Figure 5. Detail of gap formation in a sandwich pipe submitted to traction load (Case 3).

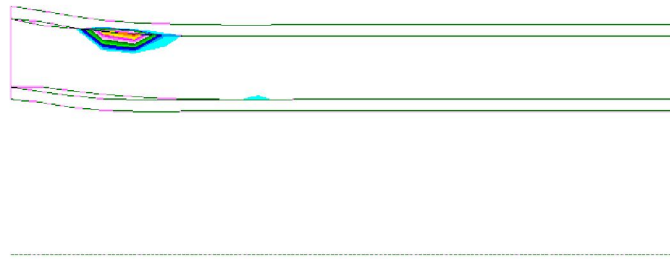


Figure 6. Friction force (0.08N) in a sandwich pipe submitted to traction load (Case 3).

## 5. CONCLUSIONS

Friction effects appear only in regions where there is slip between layers and, in this case study, this seems to be more pronounced in regions where there is a sudden change (along the longitudinal axis) from gap regions to contact regions, which may be caused by border effects. In Figure 6, it is possible to notice that the friction region is in fact very small, so it has a minor impact on the pipe global behavior. Also, from Tables 4 and 5, it is possible to observe that the possibility of gap formation between layers may be more relevant than consideration of friction effects. The most remarkable effect related to Cases 2 and 3 (unbounded layers) is the introduction of an asymmetry in the stiffness matrix  $K$ . In spite of that, the equivalent axial stiffness value of the pipe,  $(EA)_{eq}$ , does not vary significantly, what means that the global behavior of the pipe does not seem to be affected by nonlinear effects as gap formation or friction between layers (at least under the given conditions).

Since the differences between equivalent values for all the four conditions are very small, the hypotheses used in the analytical prediction can be used without losses in the results, what means that simplified analytical models can provide good results even for unbounded tubes, when considering only axial loads. The friction effects in unbounded pipes are also irrelevant for the global structural behavior and it can be safely neglected.

## 6. ACKNOWLEDGEMENTS

The authors would like to thank the University of São Paulo, FAPESP (the State of São Paulo Research Funding Foundation) and CNPq (the National Research Council) for the invaluable support to their research activities.

## 7. REFERENCES

- Love, A.E.H., 1944, "A Treatise on the Mathematical Theory of Elasticity", 4<sup>th</sup> ed., Dover Publications, 643 p.
- Sokolnikoff, I.S., 1956, "Mathematical Theory of Elasticity", 2<sup>nd</sup> ed., McGraw-Hill, New York, 476 p.
- Timoshenko, S.P. and Goodier, J.N., 1970, "Theory of Elasticity", 3<sup>rd</sup> ed., McGraw-Hill, New York, 567 p.
- Castello, X. and Estefen, S.F., 2007, "Limit strength and reeling effects of sandwich pipes with bonded layers", International Journal of Mechanical Sciences, Vol. 49, Rio de Janeiro, Brazil, pp. 577-588.
- Estefen, S. F., Netto, T.A., Pasqualino, I. P., 2005, "Strength Analyses of Sandwich Pipes for Ultra Deepwaters", Journal of Applied Mechanics, Vol. 72, Rio de Janeiro, Brazil, 599 p.
- Ramos Jr, R., Martins, C. A., Pesce, C. P., Roveri, E. F., 2008, "A Case Study on the Axial-Torsional Behavior of Flexible Risers", Proc. of the ASME 27<sup>th</sup> OMAE.

## 8. RESPONSIBILITY NOTICE

The authors are the only responsible for the printed material included in this paper.